Segmental orientation in model networks of poly(dimethylsiloxane): Fouriertransform infrared dichroism measurements and theoretical interpretation

ARTICLE *in* MACROMOLECULES · MARCH 1992

Impact Factor: 5.8 · DOI: 10.1021/ma00033a018

7 AUTHORS, INCLUDING:

Souhail Besbes
University of Sfax
122 PUBLICATIONS **1,654** CITATIONS
SEE PROFILE

Liliane Bokobza
MINES ParisTech
123 PUBLICATIONS **2,850** CITATIONS
SEE PROFILE

Ivet Bahar
University of Pittsburgh
305 PUBLICATIONS **12,303** CITATIONS
SEE PROFILE

Burak Erman
Koc University
220 PUBLICATIONS **5,958** CITATIONS
SEE PROFILE

Segmental Orientation in Model Networks of Poly(dimethylsiloxane): Fourier Transform Infrared Dichroism Measurements and Theoretical Interpretation

S. Besbes, I. Cermelli, L. Bokobza,* and L. Monnerie

Laboratoire de Physico-Chimie Structurale et Macromolêculaire, ESPCI, 10 rue Vauquelin, 75231 Paris Cédex 05, France

I. Bahar and B. Erman

Polymer Research Center and School of Engineering, Bogazici University, Bebek 80815, Istanbul, Turkey

J. Herz

Institut Charles Sadron (CRM-EAHP), 6 rue Boussingault, 67083 Strasbourg, France

Received June 3, 1991; Revised Manuscript Received December 16, 1991

ABSTRACT: Segmental orientation in model networks of poly(dimethylsiloxane) (PDMS) in uniaxial tension is measured by infrared dichroism. Measurements are made on four tetrafunctional end-linked networks having molecular weights of 2×10^3, 5×10^3, 10×10^3, and 23×10^3 between junctions. Results of experiments are compared with predictions of calculations based on (i) the widely used Kuhn expression and (ii) the rotational isomeric state formalism. The Kuhn expression is found to considerably overestimate the segmental orientation of the PDMS chains. The rotational isomeric state approach leads to values of segmental orientation that fall between predictions of the affine and phantom network models. This indicates that nematic-like intermolecular contributions to orientation are not significant.

Introduction

Various spectroscopic techniques such as fluorescence polarization, nuclear magnetic resonance, and infrared dichroism are increasingly being used to study segmental orientation in deformed polymeric networks.[1] These techniques directly probe the orientational behavior of network chains at the molecular level and are therefore superior to indirect estimates of segmental orientation based on macroscopic measurements of stress and strain. The use of spectroscopic techniques on well-defined model networks readily allows for a lucid understanding of chain behavior at the microscopic level.

In general, segmental orientation with respect to a preferential orientational axis may be expressed in terms of the second Legendre polynomial $P_2(\cos \vartheta)$ as[1,2]

$$S = \langle P_2(\cos \vartheta) \rangle = 3 \langle \cos^2 \vartheta \rangle / 2 - 1/2 \qquad (1)$$

Here ϑ is the angle between the directional vector **u** characteristic of a given chain segment and the preferential orientation axis which may be taken as the laboratory-fixed Z axis, as shown in Figure 1. The angular brackets refer to the ensemble averaging over all segments in a given chain and over all possible configurations for the latter. In the case of a network chain subject to uniaxial elongation, the preferential direction coincides with that of the extension. The chain segment may be identified with portions of the chain ranging from a single bond to a few monomeric units, depending on the vectorial quantity probed by the specific experimental technique.

The present paper is devoted to the analysis of molecular orientation of model networks of poly(dimethylsiloxane) (PDMS) by infrared dichroism. PDMS chains exhibit distinctive properties such as low glass transition temperature and very high chain flexibility. Their relatively low viscosity at ordinary temperatures makes possible the network-forming reaction even in the bulk. The behavior of PDMS networks subject to uniaxial extension has already been investigated by deuterium nuclear magnetic resonance[3–6] and by small-angle neutron scattering.[7,8] These experiments have been performed on the same type of model networks as those used in the present study. The advantages of using model networks have been widely discussed.[9,10] Recent developments in network synthesis allow for the preparation of nearly ideal end-linked networks of controlled polydispersity, with junctions of almost constant functionality. Defects such as dangling chains, loops, or double connections are generally small in model networks.[11]

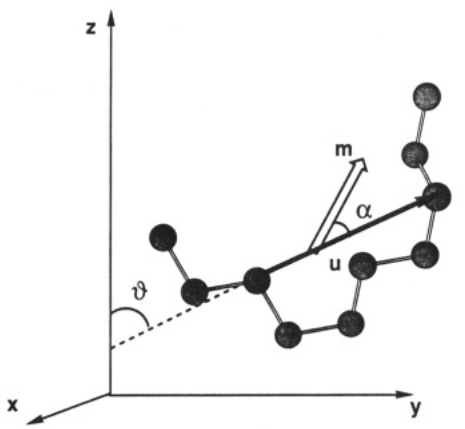

Figure 1. Portion of a chain showing the direction **u**, the transition moment **m**, and the laboratory-fixed system $OXYZ$. The Z direction is the preferential direction. The angle between **u** and **m** is α, and the angle between **u** and the preferential direction is ϑ. For the PDMS network subject to uniaxial tension, **u** is chosen to lie along the line joining two successive oxygen atoms, $\alpha = 90°$, and the preferential direction is that of stretch of the network.

In the next section we report the results of Fourier transform infrared dichroism measurements in model PDMS networks under uniaxial tension. Theoretical approaches to treat segmental orientation in deformed

0024-9297/92/2225-1949$03.00/0

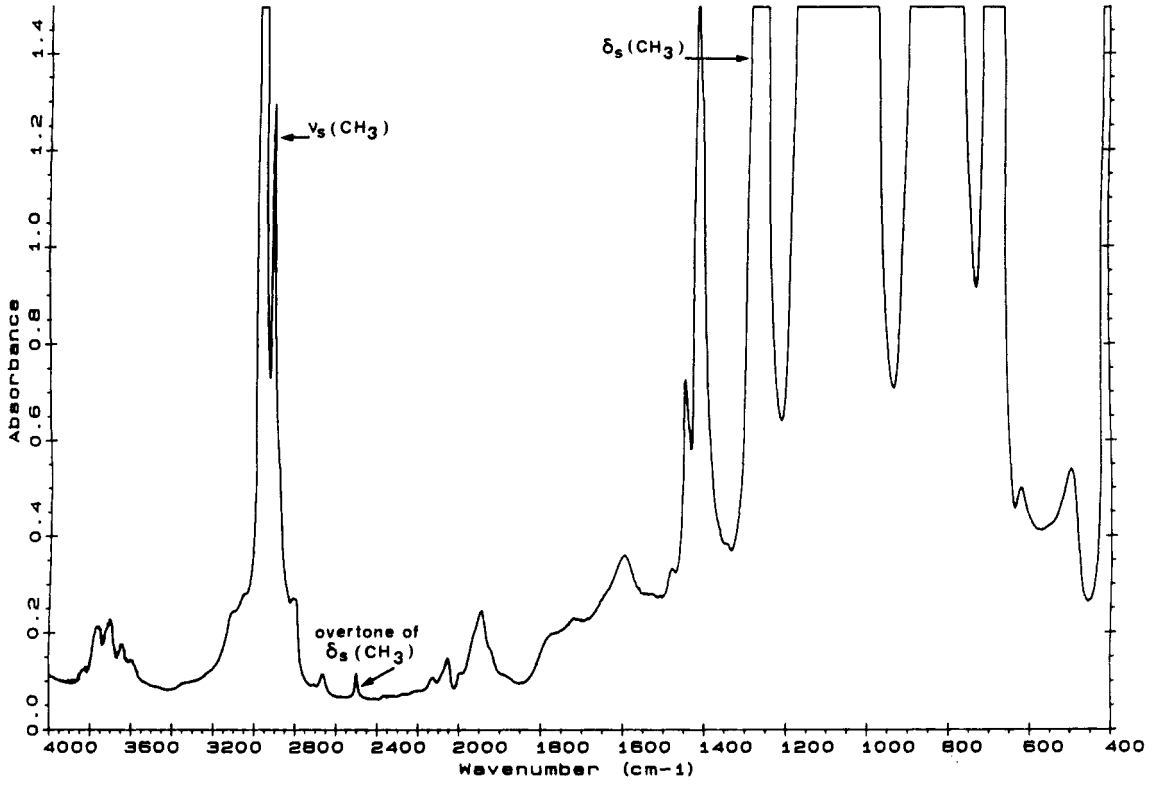

Figure 2. Infrared spectrum of PDMS films.

networks are presented in the succeeding section. The use of monodisperse chains in the preparation of the networks permits a quantitative comparison with theoretical predictions, as will be presented in the calculations and comparison with experiments section below. Results and conclusions are discussed in the final section.

Experiments

Synthesis of Model Networks. End-linking processes using α,ω-bifunctional polymers of known molecular weight reacting with adequate multifunctional reagent lead to well-defined elastomeric networks with structures as close as possible to ideality. In the present work, model networks were obtained by reacting stoichiometric mixtures of precursor chains of α,ω-di(hydrogeno)-poly(dimethylsiloxane) with 1,3,5,7-tetravinyl-1,3,5,7-tetramethylcyclotetrasiloxane, used as a tetrafunctional cross-linking agent. Precursor polymers, covering a molecular weight range from 2000 to 23 000 were kindly supplied by Rhône-Poulenc Industries (Silicone Division). The molecular weights M_c of network chains between junctions are equal to those of the precursor chains. The syntheses were performed in the bulk in the presence of chloroplatinic acid (H_3PtCl_6) used as a catalyst. The reacting mixture was cast onto a Teflon plate, and the reaction was carried out there at 80 °C for 5–10 h. The sol fractions of the samples were between 3 and 8% for M_n going from 2000 to 23 000. The thickness of the films varied between 100 and 300 μm.

Deformation and Infrared Measurements. Network elongation was performed as described earlier.[12] Infrared spectra were obtained with a Fourier transform infrared (FTIR) Nicolet 7199 spectrometer, using a resolution of 2 cm^{-1} and a number of scans of 100. The effect of anisotropy on a selected absorption band of the infrared spectrum of the sample is characterized by the dichroic ratio R, defined as $R = A_\parallel/A_\perp$, $A_\parallel$ and $A_\perp$ being the absorbances measured with radiation polarized parallel and perpendicular to the stretching direction, respectively. In order to avoid data dispersion, three dichroic ratios were determined and averaged for a given extension ratio λ. λ is defined as the ratio of the final length of the sample in uniaxial tension (or compression) to that in the state of reference, which may be chosen as the state at which the network is prepared.

Orientational measurements by the infrared technique require band absorbances sufficiently low to obey the Beer–Lambert law. On the other hand, the investigated vibrational bands must be well assigned in order to deduce the respective transition moment direction with respect to **u**. A chain segment of about one monomeric unit is investigated in FTIR dichroism measurements as long as the dipole moment change implied by a given infrared-active normal vibration may be conveniently described by the orientational motion of a transition moment vector **m** rigidly affixed to each repeat unit. Denoting by α the angle between the transition moment **m** in a given chain segment and the directional vector **u** characteristic of that segment, as shown in Figure 1, the segmental orientation S detected by infrared spectroscopy is expressed in terms of the dichroic ratio R as[1]

$$S = \langle P_2(\cos\vartheta)\rangle = \frac{R-1}{R+2}\,\frac{2}{3\cos^2\alpha - 1} \qquad (2)$$

for network chains subject to uniaxial deformation along the Z axis. Equation 2 implicitly assumes that the directional vector **u** is an axis of symmetry for the chain segment. For the particular case of PDMS chains presently investigated, **u** is taken along the vector joining two successive O atoms, and **m** is the resultant of two adjacent Si–CH_3 bond vectors thus lying in the plane perpendicular to **u** such that the angle α equates to 90°.

Results of Measurements. The infrared spectrum of PDMS films is shown in Figure 2. This spectrum exhibits very strong absorption bands. The dichroic behavior of the band at 2500 cm^{-1} has been examined. This band is ascribed to the overtone of the CH_3 symmetrical bending vibration located at 1260 cm^{-1}. Owing to the almost uncoupled nature of the methyl group, the transition moment direction of the CH_3 symmetrical bending mode is localized along the CH_3–Si bond. The overtone level belongs to the same symmetry species as the fundamental vibration, so the transition moment corresponding to the band located at 2500 cm^{-1} also lies along the Si–C bond direction which is a symmetry axis for the methyl group.

In Figure 3, the dichroic ratios are plotted against the extension ratios λ for four different networks with respective M_c values equal to 2×10^3, 5×10^3, 10×10^3, and 23×10^3. It can be seen that the investigated band exhibits a perpendicular dichroism.

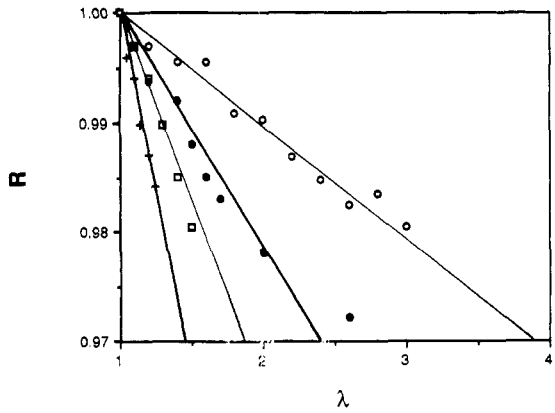

Figure 3. Dependence of dichroic ratios R on extension ratio λ for four different networks. The experimental points for the networks with $M_c = 2 \times 10^3$, 5×10^3, 10×10^3, and 23×10^3 are shown with the symbols +, □, ●, and ○, respectively. The straight lines are obtained by least-squares fit.

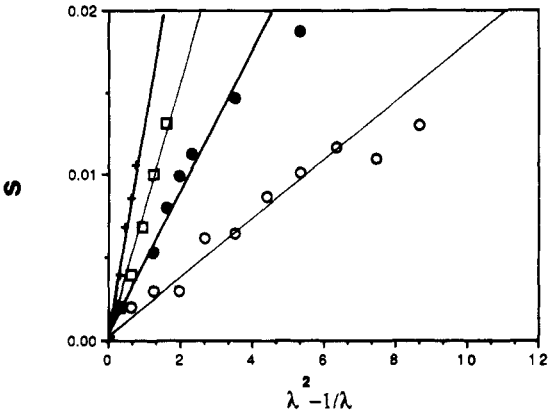

Figure 4. Dependence of the orientation function S on deformation. The ordinate values are presented as $\lambda^2 - 1/\lambda$ in order to afford comparison with eq 3 or 4. The experimental points for the networks with $M_c = 2 \times 10^3$, 5×10^3, 10×10^3, and 23×10^3 are shown with the symbols +, □, ●, and ○, respectively. The straight lines are obtained by least-squares fit.

Values of S obtained by using eq 2 for the networks prepared with the four different precursor polymers are reported in Figure 4. In order to compare the results with the predictions of eq 3 or 4 given below, S values are plotted against $\lambda^2 - 1/\lambda$. The straight lines are drawn by least-squares fit. As already observed in NMR studies,[3-6] almost linear dependences of S on $\lambda^2 - 1/\lambda$ take place in the investigated deformation range.

Theory

Precise experimental determination of segmental orientation by means of direct spectroscopic methods leads to the possibility of testing the limits of the validity of the various theoretical models used in the literature in estimating molecular orientation under deformation. In the present section, we briefly recapitulate various approaches used for the theoretical analysis of segmental orientation in a deformed network.

The orientation function S defined by eq 1 may be related to network parameters and to the state of deformation by a series expansion[13-15] whose first term reads

$$S = D_0(\lambda^2 - \lambda^{-1}) \tag{3}$$

where D_0 depends on the choice of the detailed molecular model of the network chain. Higher order serial expressions for S are given in refs 13–15. In the simplest form given by eq 3, S may be expressed as the product of two contributions: the front factor D_0, which incorporates the structural features of the specific network chain, and the strain function $(\lambda^2 - \lambda^{-1})$, which reflects the effect of the macroscopic deformation on orientation.

Equation 3 holds for the orientation in a network chain whose ends deform affinely with the macroscopic strain. In the other extreme case of phantomlike chains, the expression for the orientation function becomes[11]

$$S = D_0(1 - 2/\phi)(\lambda^2 - \lambda^{-1}) \tag{4}$$

Here ϕ is the functionality of the junctions. For the evaluation of D_0, several models of different degrees of sophistication and rigor exist in the literature, some of which will be summarized below.

The Kuhn Expression for Segmental Orientation.[16] This is the simplest expression which has found the widest use in the characterization of orientation when the state of deformation of the network is known. The network chains are assumed to consist of N freely jointed Kuhn segments. The front factor D_0 equates to

$$D_0 = 1/5N \tag{5}$$

The derivation of eq 5 is based on the assumptions that the chain ends deform affinely with macroscopic strain and intermolecular correlations are absent. A major shortcoming of the Kuhn expression for orientation is that the size of a Kuhn segment in a given real chain is not established unambiguously. For polyethylene, for example, the previous estimate of the number of bonds in a Kuhn segment is about 10,[17] while later calculations of Yoon and Flory[18] based on higher moments lead to a much larger value of 22.

The Nagai Expression for Segmental Orientation.[13,17] A general and rigorous treatment for a chain of n bonds leads in the first approximation to the following statistical average for D_0

$$D_0 = (3\langle r^2 \cos^2 \Phi\rangle_0/\langle r^2\rangle_0 - 1)/10 \tag{6}$$

where Φ is the angle between a vector affixed to a chain segment and whose orientation is being considered and the chain end-to-end vector. The angular brackets denote the ensemble average and the subscript zero indicates that averaging is performed for chains in the unconstrained state. D_0 is of the order of $1/n$ and hence constitutes the first-order approximation. The averages appearing in eq 6 may conveniently be evaluated for real chains by the rotational isomeric state (RIS) formalism.[17] Thus, within the validity of the RIS scheme, eq 6 represents the exact first-order expression. Its use instead of $1/5N$ removes the objection raised against the Kuhn model.

The moments $\langle r^2 \cos^2 \Phi\rangle_0$ and $\langle r^2\rangle_0$ in eq 6 may be evaluated either by a matrix generation technique or by Monte Carlo chain generation.[2,19] The latter has the advantage of yielding the higher order moments involved in the remaining terms of the series expansion for S, as has been recently performed.[15] In the following, the basic approach adopted for generating PDMS chains is outlined.

Statistical Characteristics of PDMS. The statistics of the PDMS chain has been investigated by various authors.[17,20-24] In order to reduce cross-referencing, we briefly summarize the basic statistical features of this system.

The first few bonds of the chain are shown in Figure 5. The chains are homologues of the series $CH_3\{Si(CH_3)_2O\}_{x_u}$-$Si(CH_3)_3$. According to the convention adopted in previous work, the chain is assumed to start and end with the silicon atom. x_u indicates the number of mers in the chain. The number of bonds n is equal to $2x_u$. The bond numbers are indicated in Figure 5. The first Si atom is taken as the zeroth atom. A laboratory-fixed coordinate system $OXYZ$

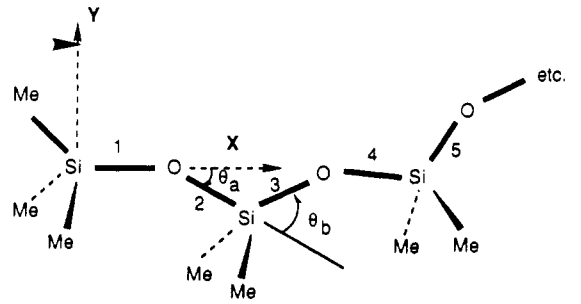

Figure 5. Schematic representation of a few bonds of the PDMS chain showing the geometrical parameters and the notation used in calculations.

is affixed to the first bond, with the Si–O bond along the X axis and the next O–Si bond in the XY plane. The length of the Si–O bond is 1.64 Å. The bond angles θ_a and θ_b are 37° and 70°, respectively. Due to the inequality of these two bond angles, the all-trans form of the PDMS chain departs from linearity and closes on itself in about 11 bonds.

The configurations of the chain are treated in terms of three rotational states accessible to backbone bonds, referred to as the trans (t), gauche$^+$ (g$^+$), and gauche$^-$ (g$^-$) states, located at rotational angles ϕ of 0°, 120°, and −120°, respectively, from the planar configuration shown in Figure 5. The statistical weight matrices for the two distinct pairs of bonds (O–Si, Si–O) and (Si–O, O–Si) are designated by $\mathbf{U}_a$ and $\mathbf{U}_b$, respectively, and equate to

$$\mathbf{U}_a = \begin{bmatrix} \tau & \sigma & \sigma \\ 1 & \sigma\psi & \sigma\omega \\ 1 & \sigma\omega & \sigma\psi \end{bmatrix} \tag{7}$$

$$\mathbf{U}_b = \begin{bmatrix} \tau' & \sigma & \sigma \\ 1 & \sigma\psi' & \sigma\omega' \\ 1 & \sigma\omega' & \sigma\psi' \end{bmatrix}$$

where the statistical weight parameters ξ ($=\sigma$, τ, τ', ω, ω', ψ, or ψ') are the Boltzmann factors given by

$$\xi = \exp(-E_\xi/RT) \tag{8}$$

For a chain of x_u repeat units the configurational partition function Z is found from the serial multiplication of the statistical weight matrices as

$$Z = \mathbf{J}^*\mathbf{U}_b(\mathbf{U}_a\mathbf{U}_b)^{x_u-1}\mathbf{J} \tag{9}$$

where $\mathbf{J}^* \equiv$ row (1, 0, 0) and $\mathbf{J} \equiv$ col (1, 1, 1). The moments $\langle r^2\rangle_0$ and $\langle r^2\cos^2\Phi\rangle_0$ in eq 6 may be evaluated using the RIS model either by the matrix generation scheme[17] or by the conditional Monte Carlo technique.

Conditional Monte Carlo Simulations. Torsional angles are assigned to successive skeletal bonds in Monte Carlo chains on the basis of conditional probabilities for the rotameric states of adjacent bonds. The conditional probability $q_{\zeta\eta;i}$ of occurrence of isomeric state η for bond i, given that bond $i-1$ is in state ζ, is found from the joint probabilities $p_{\zeta\eta;i}$ as

$$q_{\zeta\eta;i} = p_{\zeta\eta;i}/\sum_\eta p_{\zeta\eta;i} \tag{10}$$

where the summation extends over all states accessible to bond i and the joint probability $p_{\zeta\eta;i}$ of states $\zeta\eta$ for the respective bonds $i-1$ and i is evaluated from

$$p_{\zeta\eta;i} = Z^{-1}\mathbf{J}^*[\prod_{h=2}^{i-1}\mathbf{U}_h]\mathbf{U}'_{\zeta\eta;i}[\prod_{j=i+1}^{n-1}\mathbf{U}_j]\mathbf{J} \tag{11}$$

Here $\mathbf{U}'_{\zeta\eta;i}$ is the matrix obtained by equating all elements of $\mathbf{U}_i$ to zero, with the exception of the element $\zeta\eta$. Following the index notation adopted for convenience in eq 11, the matrix $\mathbf{U}_2$ is identified with $\mathbf{U}_b$, $\mathbf{U}_3$ with $\mathbf{U}_a$, ..., $\mathbf{U}_{n-1}$ with $\mathbf{U}_b$. The use of distinct conditional probabilities for each bond i in a given chain is important in short chains whereas end effects are vanishingly small for chains of about $n > 40$.

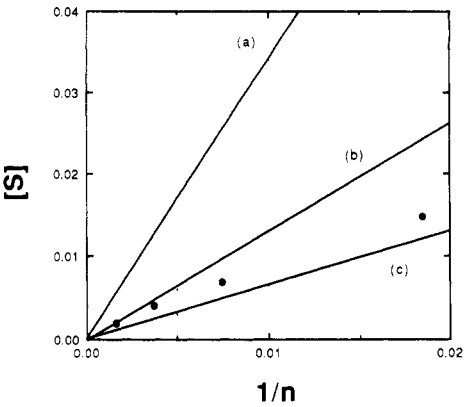

Figure 6. Comparison of the experimentally determined reduced orientation function with theoretical expressions. The abscissa shows the reciprocal of the number of bonds. The circles represent experimental data. The straight lines are from eq 13 for (a) Kuhn, (b) Nagai–affine network, and (c) Nagai–phantom network models.

Calculations and Comparison with Experiments

The approximate linear relationship between the experimentally observed S values and $\lambda^2 - 1/\lambda$ in Figure 4 indicates that segmental orientation in uniaxial extension obeys the strain dependence given by eq 3 or 4. No recourse to higher order approximation in the serial expression for S is required, since experimental data points are rather scattered to justify a more refined approach. Having thus confirmed the functional form of these equations, the fundamental problem that remains is the quantitative estimation of the front factor. This may be conveniently done by introducing the reduced orientation defined by

$$[S] = S/(\lambda^2 - 1/\lambda) \tag{12}$$

With this definition, the reduced orientation equates to the slope of the best fitting straight lines shown in Figure 4. For the various theoretical expressions, $[S]$ takes the following simple forms:

$$[S] = \begin{cases} 1/5N & \text{(a)} \\ (3\langle r^2\cos^2\Phi\rangle_0/\langle r^2\rangle_0 - 1)/10 & \text{(b)} \\ (1 - 2/\phi)(3\langle r^2\cos^2\Phi\rangle_0/\langle r^2\rangle_0 - 1)/10 & \text{(c)} \end{cases} \tag{13}$$

The above identities correspond to (a) the Kuhn expression, (b) the Nagai formulation for affine networks, and (c) the Nagai formulation adopted for phantom networks. Values of the reduced orientation experimentally found for the four different size network chains are compared in Figure 6 with the theoretical expressions of eq 13. The ordinate represents the reduced orientation and the abscissa is the reciprocal of the number of bonds. The points represent experimental data. The curves display the results from the three theoretical approaches a, b, and c, as indicated.

Inasmuch as the PDMS chain does not assume a rectilinear form in the planar all-trans configuration, it is not possible to estimate N by simply comparing the fully stretched lengths of the real chain and the equivalent Kuhn chain. Instead, this value is found by Flory and Chang[22]

Table I
Results of Monte Carlo Calculations

no. of bonds	$\langle r^2 \rangle_0$	$\langle r^2 \cos^2 \Phi \rangle_0$	$D_0 \times 10^{-2}$
20	250.6	136.8	6.375
50	690.6	292.2	2.691
100	1415.0	533.5	1.307
200	2800.0	990.0	0.607

through comparison of the higher moments of a real PDMS chain of a given number of bonds with those of a freely jointed one. Accordingly, the number of bonds in a Kuhn segment is obtained as 17. Adoption of this value leads to the higher straight line in Figure 6. As a result, the experimental data points are about 3 times lower than the predictions of the Kuhn expression.

The intermediate curve b is obtained from the affine model of orientation given by the second line of eq 13. The lower curve c follows from the phantom model with $\phi = 4$, represented by the third line of eq 13. The Monte Carlo chain generation technique has been employed in both cases to evaluate the averages in eq 13. Calculations were performed for chains of $n = 20$, 50, 100, and 200 bonds, at 20 °C.

Two different sets of data were considered for the intramolecular energies associated with the statistical weight parameters: The former, introduced by Crescenzi, Mark, and Flory, takes $E_\sigma = 0.30$ kcal/mol, $E_{\omega'} = 1.05$ kcal/mol, and $E_\omega = \infty$, with all other energy parameters equated to zero. A more recent work by Bahar and Mattice,[24] proposed on the basis of ab initio and molecular dynamics simulations and macrocyclization equilibrium data of PDMS, adopts the set $E_\sigma = 0.30$, $E_\tau = 0.35$, $E_{\tau'} = 0.10$, $E_\omega = 0.60$, $E_{\omega'} = 0.35$, $E_\psi = 0.25$, and $E_{\psi'} = 0.20$ kcal/mol. The present results are not significantly altered with the choice of energy parameters. Nevertheless, the second set of energy parameters was found to favor more gauche placements compared to the previous model, leading to a more uniform distribution of isomeric states. As a consequence, segmental orientation is closer to random and the resulting orientation function is about 15% lower than the one obtained with the former set of energy parameters. The curves b and c displayed in Figure 6 represent the results from the second set of energy parameters.

Using the vectors $\mathbf{r}_i$ from the zeroth to the ith atom along the chain, the following variables were recorded for each Monte Carlo chain:

$$\cos \Phi_k = (\mathbf{u}_k \cdot \mathbf{r}_n)/(|\mathbf{u}_k||\mathbf{r}_n|) \tag{14}$$

where the local chain axis of the kth segment $\mathbf{u}_k$, $1 \le k \le n/2 - 1$, is found from

$$\mathbf{u}_k = \mathbf{r}_{2k+1} - \mathbf{r}_{2k-1} \tag{15}$$

The average over all segments of a given chain reads

$$\overline{r^2 \cos^2 \Phi} = (\sum_{k=1}^{n/2-1} r^2 \cos^2 \Phi_k)/(n/2 - 1) \tag{16}$$

Performing this calculation for all of the generated chains yields the required moments $\langle r^2 \rangle_0$ and $\langle r^2 \cos^2 \Phi \rangle_0$ for a given chain length. The number of chains generated was chosen so that all average quantities calculated in two different sets of Monte Carlo runs were within 2% of each other. In the present calculations, generation of 10 000 chains was sufficient.

Discussion

The fact that the experimental data points lie between the predictions of the affine and the phantom network models reminds one of the stress–strain relations where the experimentally observed moduli similarly fall between the predictions of the two models. This behavior is predicted by the constrained junction or constrained chain models, according to which the chain end-to-end vectors transform nonaffinely with macroscopic strain.[11] Previous neutron scattering[7,8] experiments and their comparison[25] with theoretical models show that the transformations of PDMS chains are remarkably close to those of the phantom model. The results for segmental orientation in PDMS are also in close agreement with predictions of the phantom network model as seen from Figure 6. It is observed that segmental orientation approaches the affine limit as the network chains get longer. This behavior is in agreement with the predictions of the constrained junction or constrained chain theories[28,29] according to which the fluctuations of chains relative to those of the phantom network decrease with increasing chain length and the network behavior approaches that of the affine network.

Results of measurements shown in Figure 6 and their close agreement with predictions of models based on single-chain statistics show that the effects of nematic-like intermolecular interactions are absent among neighboring PDMS chains. It is interesting to note that recent deuterium NMR experiments by Deloche et al.[4] indicate that free chains dissolved in a deformed network exhibit the same segmental orientation as that of the network chains. The latter is attributed to strong intermolecular coupling of the free chains to the neighboring strained network chains. Although such a strong intermolecular coupling may be operative for free chains embedded in a polymer matrix, the behavior of network chains in PDMS may not be equally affected by neighbor correlations, as the present analysis indicates. The role of steric and thermotropic interactions in determining segmental orientation in deformed networks has been theoretically investigated in a recent study. Accordingly, intermolecular interactions become important with increasing chain stiffness.[26,27]

In general, swelling of networks with anisotropic solvents is expected to decrease segmental orientation due to interchain effects. Infrared dichroism measurements seem to be the most suitable technique of determining the effect of swelling on segmental orientation, and experiments along these lines are under way in our laboratories.

Calculations performed but not reported in the present study show that the contributions to segmental orientation from higher order terms in the extension ratio become very strong at larger values of deformation. As a result the S versus $\lambda^2 - 1/\lambda$ curves exhibit strong departures from linearity. Examination of Figure 4 shows that such an increase is not observed within the deformation range of the present experiments and that the linear theory is valid all throughout the applied deformation range.

It should be finally noted that, to the knowledge of the authors, the present study is the first in the literature where segmental orientation determined experimentally by a direct technique independent of foreign labels or probes compares favorably with results of rational calculations based on the detailed statistical features of the chains.

Acknowledgment. We are very much indebted to the Centre de Recherches des Carrières, Rhône-Poulenc Industries, Saint-Fons (Silicone Division), which provided us with the precursor polymers. Thanks are due especially to MM. Leising, Barthélémy and Bordone.

References and Notes

(1) Monnerie, L. *Faraday Symp. Chem. Soc.* **1983**, *18*, 1.
(2) Erman, B.; Monnerie, L. *Macromolecules* **1985**, *18*, 1985.
(3) Dubault, A.; Deloche, B.; Herz, J. *Polymer* **1984**, *25*, 1405.
(4) Deloche, B.; Dubault, A.; Herz, J.; Lapp, A. *Europhys. Lett.* **1986**, *1*, 629.
(5) Dubault, A.; Deloche, B.; Herz, J. *Macromolecules* **1987**, *20*, 2096.
(6) Sotta, P.; Deloche, B.; Herz, J.; Lapp, A.; Durand, D.; Rabadeux, J.-C. *Macromolecules* **1987**, *20*, 2769.
(7) Beltzung, M.; Picot, C.; Rempp, P.; Herz, J. *Macromolecules* **1982**, *15*, 1594.
(8) Beltzung, M.; Picot, C.; Herz, J. *Macromolecules* **1984**, *17*, 663.
(9) Herz, J. E.; Belkebir-Mrani, A.; Rempp, P. *Eur. Polym. J.* **1973**, *9*, 1165.
(10) Herz, J. E.; Rempp, P.; Borchard, W. *Adv. Polym. Sci.* **1977**, *26*, 105.
(11) Mark, J. E.; Erman, B. *Rubberlike Elasticity: A Molecular Primer*; Wiley-Interscience: New York, 1988; p 196.
(12) Amram, B.; Bokobza, L.; Queslel, J. P.; Monnerie, L. *Polymer* **1986**, *27*, 877.
(13) Nagai, K. *J. Chem. Phys.* **1964**, *40*, 2818.
(14) Roe, R. J.; Krigbaum, W. R. *J. Appl. Phys.* **1964**, *35*, 2215.
(15) Erman, B.; Haliloglu, T.; Bahar, I.; Mark, J. E. *Macromolecules* **1991**, *24*, 901.
(16) Kuhn, W.; Grün, F. *Kolloid-Z.* **1942**, *101*, 248.
(17) Flory, P. J. *Statistical Mechanics of Chain Molecules*; Interscience: New York, 1969.
(18) Yoon, D. Y.; Flory, P. J. *J. Chem. Phys.* **1974**, *61*, 5366.
(19) Erman, B.; Bahar, I. *Macromolecules* **1988**, *21*, 452.
(20) Flory, P. J.; Crescenzi, V.; Mark, J. E. *J. Am. Chem. Soc.* **1964**, *86*, 138.
(21) Flory, P. J.; Semlyen, J. A. *J. Am. Chem. Soc.* **1966**, *88*, 3209.
(22) Flory, P. J.; Chang, W. C. *Macromolecules* **1976**, *9*, 33.
(23) Bahar, I.; Zuniga, I.; Dodge, R.; Mattice, W. L. *Macromolecules* **1991**, *24*, 2986.
(24) Bahar, I.; Zuniga, I.; Dodge, R.; Mattice, W. L. *Macromolecules* **1991**, *24*, 2993.
(25) Erman, B. *Macromolecules* **1987**, *20*, 1917.
(26) Erman, B.; Bahar, I.; Kloczkowski, A.; Mark, J. E. *Macromolecules* **1990**, *23*, 5335.
(27) Bahar, I.; Erman, B.; Kloczkowski, A.; Mark, J. E. *Macromolecules* **1990**, *23*, 5341.
(28) Flory, P. J.; Erman, B. *Macromolecules* **1982**, *15*, 800.
(29) Erman, B.; Monnerie, L. *Macromolecules* **1989**, *22*, 3342.

Registry No. 1,3,5,7-Tetravinyl-1,3,5,7-tetramethylcyclotetrasiloxane, 2554-06-5.